Hyaluronic acid-based hydrogels with independently tunable mechanical and bioactive signaling features

Madison D. Godesky, and David I. Shreiber

Citation: Biointerphases **14**, 061005 (2019); doi: 10.1063/1.5126493
View online: https://doi.org/10.1063/1.5126493
View Table of Contents: https://avs.scitation.org/toc/bip/14/6
Published by the American Vacuum Society

Hyaluronic acid-based hydrogels with independently tunable mechanical and bioactive signaling features

Madison D. Godesky and David I. Shreiber[a)]
Department of Biomedical Engineering, Rutgers, The State University of New Jersey, 599 Taylor Road, Piscataway, New Jersey 08854

(Received 3 September 2019; accepted 19 November 2019; published 2 January 2020)

Extracellular matrix provides critical signaling context to resident cells through mechanical and bioactive properties. To realize the potential of tissue engineering and regenerative medicine, biomaterials should allow for the independent control of these features. This study investigates a hydrogel system based on thiol-modified hyaluronic acid (HA-S) and polyethylene glycol diacrylate (PEGDA). The mechanical properties of HAS-PEGDA are dictated by two cytocompatible crosslinking reactions that occur at distinct time points: a rapid, Michael-type nucleophilic addition reaction between HA-thiols and PEG-acrylates and a prolonged maturation of disulfide crosslinks from remaining thiols. It is hypothesized that these reactions would enable the independent tuning of the mechanical and bioactive features of HAS-PEGDA. Rheological studies confirmed that initial gelation reached completion by 1 day, at which point the shear modulus was proportional to the concentration of PEGDA. Over time, the shear modulus evolved dramatically, and final stiffness depended on the availability of HA-thiols. The addition of PEG-monoacrylate (PEGMA) after the initial gelation occupied a percentage of remaining thiols to prevent disulfide crosslinking, decreasing the steady-state stiffness in a dose-dependent manner. A fraction of the PEGMA was then replaced with acrylated peptide ligands to introduce specific bioactivity to the otherwise non-cell-adhesive network. The degree of latent stiffening was controlled by the total amount of peptide-PEGMA, while adhesivity was tuned with the balance of bioactive and inactive peptides. The functional effects of the tunable mechanical and bioadhesive ligand properties were confirmed with assays of cell adhesion and morphology. *Published by the AVS.*
https://doi.org/10.1063/1.5126493

I. INTRODUCTION

Bioengineered tissues offer significant therapeutic potential in regenerative medicine and value as *in vitro* tools for basic research, product development, and precision and personalized medicine, especially with the advent of 3D bioprinting.[1] However, bioengineered tissues require materials to create an initial signal context for cells to maintain their programmed functions and coordinate the formation of tissues.[2] One promising source or inspiration for materials is extracellular matrix (ECM).

During tissue development and regeneration, cell functions are coordinated through a series of fate decisions directed in part by matrix-bound guidance signals.[3] Cells respond to ligands presented in the ECM according to the type, number, and distribution of receptors they express. Inside the cell, receptor-ligand interactions trigger signal cascades that can regulate gene expression and integrate multiple external cues into a single programmed response.[4] At the tissue level, ECM-bound ligands serve as positional controls and influence tissue shape as their presentations change over time.[5] For instance, the density and specificity of adhesive ligands can recruit certain cell types to precise spatial locations.[6–12] Additionally, in the absence of adhesive interactions, anchorage-dependent signaling can trigger apoptosis, ensuring that only specific cell types can survive in particular anatomical positions.[3,13]

In addition to ligand-initiated molecular signaling, adhesive complexes transmit mechanical forces between cells and the ECM.[14–19] Cells generate traction forces between membrane integrins and adhesive ligands as they move. Depending on the stiffness of the ECM and the distribution of adhesion sites, traction forces differentially regulate cell shape and gene expression.[18–23] Through mechanotransduction, cells interpret changes in matrix stiffness as alterations in adhesive ligand density.[14,18] Mechanical forces not only act on cells, but they also reorganize the matrix. Through remodeling, ECM can propagate signals from cell-to-cell,[3] dictate tissue orientation,[24] and provide feedback across multiple time and length scales.[5,16]

While adhesive ligands are critical to the regulatory functions of most ECM molecules, they often complicate the use of ECM or ECM derivatives for tissue engineering. From an engineering perspective, non-cell-adhesive materials are advantageous to pattern specific ECM features while limiting nonspecific cellular interactions,[25] which precludes most native biomaterials. One notable exception is hyaluronic acid (HA).[26–31] Structurally, HA is one of the simplest ECM components; it is a linear, unbranched, and regularly repeating glycosaminoglycan (GAG). Unlike other GAGs, HA lacks thiol-functionality and covalent linkages to specific

[a)]Electronic mail: shreiber@soe.rutgers.edu

core proteins.[13] Since HA's GAG chain is negatively charged, it attracts cations and water and swells to fill large volumes.[13] During morphogenesis, for example, the swelling of HA forces physical changes to the shape and the structure of developing tissues. Stem cells produce HA to create open, hydrated, and cell-free spaces for specific progenitors to infiltrate.[3] HA's water content also enables it to resist compaction forces from cell movement and, thus, maintain the tissue shape as cells migrate.[13,32] Once migration ends, such as in the formation of the heart, cornea, and several other organs,[3] cells degrade HA with hyaluronidase to create space for new ECM molecules.[18,26,27]

Although native HA has many advantages, bioengineering applications have been restricted because of its weak mechanical properties when isolated from the rest of the ECM.[30,33] Thiol-modified hyaluronic acid (HA-S) crosslinked with polyethylene glycol diacrylate (PEGDA) is a hydrogel-forming biomaterial that presents many attractive characteristics of native HA with a convenient mechanism to improve its mechanical properties.[30] In contrast to many hydrogel systems that rely on a single gelation reaction, the mechanical properties of HAS-PEGDA are dictated by two crosslinking reactions that occur at different time points.[33] The first crosslinking mechanism is a Michael-type nucleophilic addition reaction between HA-thiols and PEG-acrylates and results in the material's gelation in minutes.[34] After initial gelation, the remaining thiols on HA can then form disulfide crosslinks upon oxidation.[30] Although disulfide crosslinking is considerably slower than initial gelation, it dramatically stiffens the hydrogel over time.[33] Furthermore, HA-thiols provide convenient targets to introduce bioadhesive ligands. However, consuming thiols will naturally affect the resultant stiffness of the network.

In the current study, we investigate several strategies to decouple and tune the stiffness and adhesive ligand conditions presented in HAS-PEGDA hydrogels. By leveraging the dual crosslinking mechanism, we establish a system to independently control the mechanical and bioactive features across multiple time scales. Enabling control over stiffness and adhesion would have a great value for applications across tissue engineering and regenerative medicine, especially in 3D bioprinting, where different inks may be combined at specific locations to spatially control tissue composition and behavior.

II. EXPERIMENT

A. Rheology

Hydrogel samples were prepared in Petri dishes, and the rheological properties were measured over long curing times using a Kinexus Ultra Rotational Rheometer (Malvern Panalytical Ltd., Malvern, UK) equipped with a 3D-printed lower geometry and a 20 mm parallel upper plate. HA-S (Glycosil®, BioTime, Inc., Alameda, CA) and PEGDA (MW 3.4 kDa, Laysan Bio Inc., Arab, AL) were purchased commercially, and stock solutions containing 1.25% HA-S and 4% PEGDA (%w/v) were prepared in de-ionized water according to the manufacturer's instructions.[35] Stock solutions of HA-S and PEGDA were diluted serially and mixed in 4:1 volumetric ratios to achieve the indicated final concentrations of HA-S (0.8% or 1.0%) and PEGDA (0.2% or 0.6%). Circular hydrogel samples of 0.2 mL HAS-PEGDA were formed in Petri dishes containing annular molds of PDMS (id = 20 mm), covered with 0.01 M phosphate buffered saline solution (1× PBS) after 2 h of gelation, and incubated at 37 °C. Gels were matured for 30 days and removed from the incubator periodically to assess the shear storage modulus (G') by exposing the gels to an oscillatory shear strain of 0.5% at a frequency of 1 rad/s. Unless otherwise stated, results are presented as mean ± SD of $n \geq 4$ sample replicates.

B. Tuning the rate of latent crosslinking

To accelerate latent crosslinking, dimethyl sulfoxide (DMSO), a mild oxidant,[36,37] was used. Briefly, hydrogel samples of 0.8% or 1.0% HA-S and various concentrations of PEGDA crosslinker (0.2%–1.0%) were prepared, and G' was measured after 1 day of gelation as described above. After initial testing, the samples were covered with 0.01 M phosphate buffer containing 20% DMSO (%v/v) and incubated at 37 °C and 5% CO_2. After 3 days of thiol oxidation, rheological measurements were repeated. Significant differences in G' at steady-state between gels that had been oxidized for 3 days with the oxidation medium or 30 days with ambient oxygen were identified with t-tests ($p < 0.05$).

C. Tuning the extent of latent crosslinking

Hydrogels containing 0.8% HA-S and 0.2% PEGDA were prepared as described above and allowed to mature for 1 day of gelation. To selectively block latent stiffening, solutions of 1 mL PEG-monoacrylate (PEGMA) (MW 4.8 kDa, Laysan Bio, Inc., Arab, AL) diluted in PBS to 0.05, 0.1, 0.2, 0.3, 0.6, 1.2, or 12 mM were diffused through the 0.2 mL hydrogels. After 2 days of reaction, PEGMA solutions were replaced with an oxidation buffer containing 20% DMSO, and the rheological properties were measured at steady-state. For simplicity, the total amount of PEGMA applied to each hydrogel condition (micromoles) is reported as a relative concentration with respect to the volume of the hydrogel sample (0.2 mL). In separate experiments, fluorescein-*o*-acrylate (Millipore Sigma, St. Louis, MO), a thiol-reactive and fluorescent molecule, was incorporated in the place of PEGMA to confirm that the changes in mechanical properties were due to the consumption of free thiols. The mechanical properties of these gels were assessed as described above. In addition, relative fluorescence intensities ($\lambda_{ex}/\lambda_{em} = 490/520$ nm) of separate gels that had been cured in 96-well plates (50 μL/well) were detected with an Infinite® 200 PRO microplate reader (Tecan Group Ltd., Männedorf, Switzerland) after a series of 10 washes with PBS (250 μL/well) at room temperature for a minimum of 1 h per wash to remove unbound dye.

D. Peptide functionalization

A fibronectin-derived bioactive adhesive peptide (GRGDS) and an inactive reverse sequence (SDGRG) were purchased commercially (Bachem Americas, Inc., Torrance, CA) and functionalized with acrylate reactive groups using acrylate-PEG-succinimidyl valerate (PEGMA-SVA) as a molecular scaffold[38] (MW 3.4 kDa, Laysan Bio, Inc., Arab, AL). To conjugate the peptides to PEGMA, N-terminal primary amines were reacted with PEGMA-SVA in a 5:4 molar ratio (NH_2:SVA) in 0.1 M PBS at pH 8.0. After 4 h of reaction, conjugation efficiencies were estimated with fluorescamine (Millipore Sigma, St. Louis, MO) to compare primary amine content before and after the reactions.[39,40] The PEGMA-peptide conjugates were then purified with centrifugal filter units (Amicon™ Ultra-15 3 kDa MWCO, Millipore Sigma, St. Louis, MO) against picopure water, frozen at −80 °C, and lyophilized. The lyophilized products, PEGMA-GRGDS and PEGMA-SDGRG, were stored at −20 °C under argon until use.

E. Cell studies

Hydrogels containing 0.8% HA-S and various concentrations of PEGDA (0.2%, 0.4%, 0.6%, or 0.8%) were prepared in 96-well tissue culture plates (50 μL/well). After 1 day of gelation, solutions of 7.5 mM PEGMA-peptide were applied to the gels (50 μL/well) to quench remaining HA-thiols without perturbing the hydrogels' initial gelation. The ratios of bioactive ligands (PEGMA-GRGDS) and inactive, negative control sequences (PEGMA-SDGRG) were altered to manipulate bioactivity independently of the steady-state crosslinking density. In each solution, the total concentration of peptide (PEGMA-GRGDS + PEGMA-SDGRG) was provided in excess of remaining HA-thiols to block latent stiffening. After 2 days of reaction while rocking, peptide solutions were aspirated, and the gels were washed thoroughly with culture media to remove any unbound ligand, as described above. Type-I bovine collagen hydrogels (Elastin Products Company, Owensville, MO) were prepared at 2.0 mg/mL as previously described[41] and served as positive controls for adhesivity.

Rat dermal fibroblasts (RDFs) from transgenic rat pups that constitutively express green fluorescent protein (GFP) were isolated and expanded in tissue culture using complete media: DMEM (Millipore Sigma, St. Louis, MO) supplemented with 10% fetal bovine serum (Atlanta Biologicals, Flowery Branch, GA), 1% penicillin–streptomycin, and 1% L-glutamine.[41] At approximately 90% confluency, RDFs were detached with trypsin–ethylenediaminetetraacetic acid (EDTA), pelleted, and resuspended to 25 000 cells/mL in culture media. Cells were seeded on all hydrogels using an automated, 96-channel, high-throughput transfer pipet (VIAFLO 96, Integra Biosciences Corp., Hudson, NH) to achieve a uniform final seeding density of 5000 cells/well. RDFs were incubated at 37 °C and 5% CO_2 prior to adhesion and spreading assays.

F. Adhesion and spreading assays

After 2 h of incubation, cell suspensions were aspirated from the gels, and nonadherent cells were removed with two additional washes with culture media. Concentrations of live, adherent cells were estimated with fluorescence intensity measurements ($\lambda_{ex}/\lambda_{em}$ = 488/520 nm) of constitutively expressed GFP. Cells were then incubated overnight to allow for spreading to occur. After 1 day *in vitro*, adherent RDFs were fixed with 4% paraformaldehyde and permeabilized with Triton-X. Nuclei were stained with DAPI, and F-actin was stained with TRITC-phalloidin (MilliporeSigma, St. Louis, MO). Fluorescence images in each of the three channels were taken with a 10× objective lens from at least three positions in each well using an Olympus IX81 inverted microscope (Olympus, Melville, NY). To determine the number of cells, DAPI-labeled nuclei were identified and counted using the built-in cell counter tool in FIJI (FIJI is just ImageJ, Dresden, Germany).[42] To evaluate cell spreading, images of RDF cell bodies (GFP channel) were converted to binary image masks by applying an Otsu threshold filter, and the confluency in each image was estimated with the built-in particle analysis function.[42] The average cell spreading area in each image field (μm^2/cell) was estimated by normalizing the percent confluency (GFP channel) to the corresponding cell count (DAPI channel) for each image, and then scaling this ratio to the image area (μm^2). Cell morphologies were classified as round, partially spread, or spread for areas of 250–500 μm^2, 500–750 μm^2, or >750 μm^2, respectively.

III. RESULTS AND DISCUSSION

A. Mechanical properties evolve across multiple time scales

To characterize the dual crosslinking system, rheological properties were monitored over long curing times from hydrogels containing various amounts of HA-S and PEGDA. In all hydrogel formulation conditions studied, HA-thiols (0.9 μmol thiol/mg HA-S) were presented in molar excess of PEG-acrylates (0.6 μmol acrylate/mg PEGDA). Consistent with previous reports,[33,34,43] rheological studies confirmed that gelation occurs in minutes; the initial crosslinking reaction plateaus by 1 day of gelation, and latent disulfide bonding dramatically stiffens the material over time (Fig. 1). In addition, at 1 day of gelation, G′ is primarily controlled by the concentration of PEGDA [Fig. 1(a)] and, thus, the extent of thiol-acrylate crosslinking.[13,33,44] For instance, in gels with the same HA-S concentration (0.8%), G′ after 1 day is significantly greater in gels crosslinked with 0.6% PEGDA than in gels crosslinked with 0.2% PEGDA ($p = 0.001$, t-test). Moreover, in gels with the same PEGDA concentration (0.2%), G′ after 1 day is not statistically different for gels with 0.8% HA-S or 1.0% HA-S ($p = 0.765$, t-test). Once disulfide crosslinking occurs, however, G′ is significantly greater in hydrogels containing 1.0% HA-S than in samples containing 0.8% HA-S ($p < 0.001$, t-test). The results also suggest that disulfide crosslinking evolves to

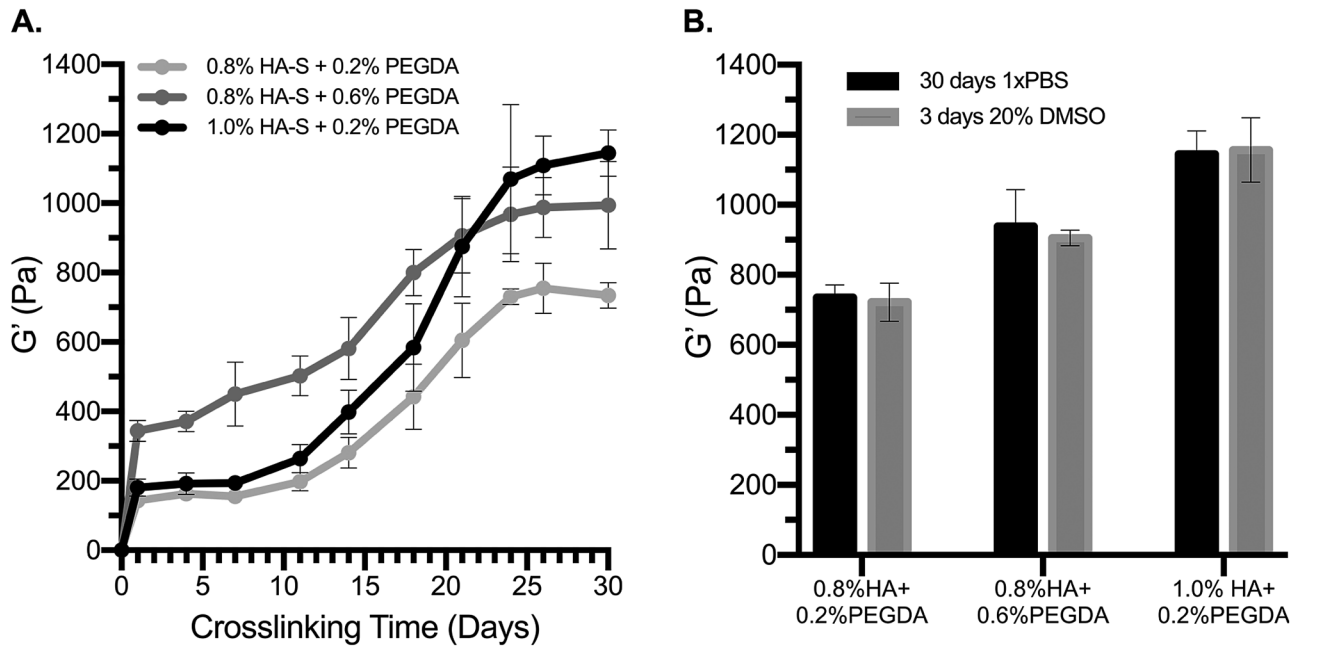

FIG. 1. Two crosslinking reactions, occurring at distinct time intervals, dictate the rheological properties of HAS-PEGDA hydrogels. (a) The initial gelation reaction between HA-thiols and PEG-acrylates plateaus before 1 day of gel maturation, and over a period of days-to-weeks, HA-thiols undergo secondary disulfide crosslinking. (b) G′ at steady-state is not significantly different when disulfide crosslinking matures in PBS for 30 days or in 20% DMSO for 3 days ($p > 0.75$, t-tests). In all conditions, G′ is presented as mean ± SEM for $n \geq 4$.

greater levels and over longer time scales than previously reported.[33,43]

B. Latent disulfide crosslinking can be accelerated with DMSO

The 30-day time frame for disulfide crosslinking is far from ideal for practical applications in the laboratory or clinic. To leverage the potential of this system, and guided by the literature,[4,36,37,45–49] we explored a number of materials that could accelerate disulfide crosslinking in HAS-PEGDA, including cysteine- and serum-free DMEM, trace amounts of H_2O_2, oxidized glutathione, and DMSO. In general, we found that thiol oxidation in the presence of 20% DMSO is rapid, is relatively mild, and produces consistent crosslinking results. Figure 1(b) demonstrates that G′ is nearly identical for gels that were matured for 30 days in PBS or for 3 days in 20% DMSO.

C. Mechanical stiffness is controllable at multiple time points

With a convenient mechanism to accelerate gel maturation, we next examined how the two crosslinking mechanisms could be targeted independently. In agreement with previous reports,[33,43] G′ is nearly linearly proportional to the PEGDA concentration ($R^2 = 0.989$) after 1 day of gelation (Fig. 2). However, at steady-state, G′ is not significantly different among gels of varying concentrations of PEGDA ($p = 0.449$, one-way ANOVA). As Fig. 2 demonstrates, hydrogels of 0.4%, 0.6%, 0.8%, and 1.0% PEGDA have relatively constant moduli at steady-state, and G′ is only slightly lower in the 0.2% PEGDA formulation condition. These findings suggest that PEGDA controls the initial stiffness of the material, but at steady-state, the mechanical properties are less tunable than previously reported.[33,43] Perhaps compounding these differences, we

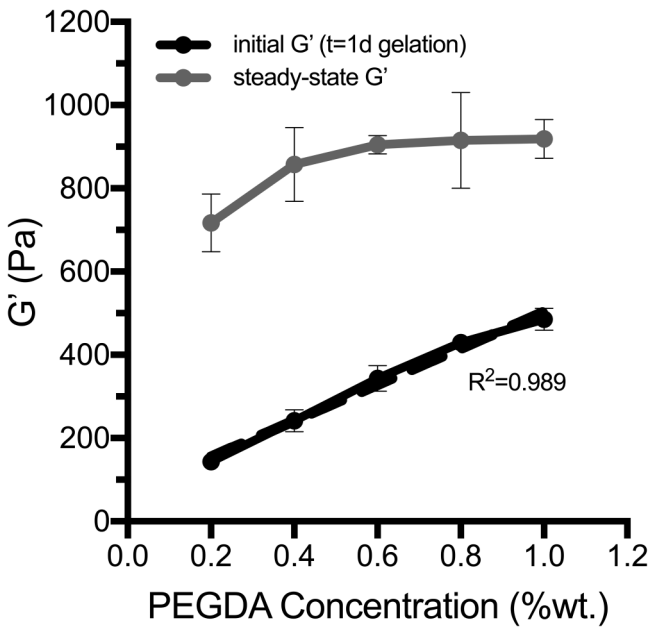

FIG. 2. Concentration of PEGDA crosslinker controls G′ after 1 day of gelation, but at steady-state, G′ depends on both the concentration of PEGDA and the availability of HA-thiols. After 1 day of gel maturation, G′ is directly proportional to the concentration of PEGDA ($R^2 = 0.989$) when HA-thiols (7.2 mM) are in molar excess of PEG-acrylates (0.6 μmol/mg of PEGDA). At steady-state, G′ is not significantly different among the different concentration conditions of PEGDA ($p = 0.449$, one-way ANOVA). In all conditions, G′ is presented as mean ± SEM for $n \geq 4$.

also found that the concentration of PEGDA influences the rate of latent stiffening; disulfides mature more rapidly in gels with higher concentrations of PEGDA. Therefore, at time points prior to the full equilibrium, differences in G′ are exaggerated by the gels' differential rates of disulfide crosslinking.

Over time, disulfide bonding significantly increases the stiffness of the hydrogels and offers a broader target range than crosslinking with PEGDA (Fig. 2). Therefore, for greater control over the equilibrium mechanical properties, we tuned the extent of latent stiffening by introducing PEGMA to occupy the sites that would otherwise form disulfide crosslinks [Fig. 3(a)]. When PEGMA is presented in excess of remaining HA-thiols, the steady-state stiffness ($G' = 141 \pm 7$ Pa) is nearly equivalent to hydrogel stiffness on 1 day of gelation ($p = 0.8267$, t-test), indicating that latent disulfide crosslinking can be completely blocked. In the same time frame, negative control gels, which were not grafted with PEGMA (0 mM), had significantly higher moduli ($G' = 812 \pm 145$ Pa, $p = 0.0013$) than gels quenched with PEGMA in excess. These results indicate that the steady-state mechanical properties can be tuned independently of initial gelation by grafting specific concentrations of thiol-reactive molecules after 1 day of gel maturation.

Similar to the rate trends discussed above with PEGDA, we also observed faster rates of disulfide crosslinking when PEGMA was incorporated into the network. Previous studies by Ghosh *et al.* report an apparent "zipping effect"[33] in which the authors suggest that PEGDA concentration controls the relative proximities of free thiols in the hydrogel network and, thus, their tendency to form disulfide crosslinks. In addition to a possible proximity effect, our findings suggest that the PEG chain, itself, may accelerate disulfide bonding independently of the initial crosslinking density that is driven by PEGDA. Although the mechanism by which this occurs is out of the scope of this work, noncovalent interactions are known to influence the rate of disulfide bond formation.[4,47,50,51] In preliminary studies, we observed faster rates of disulfide crosslinking in conditions that lowered the strength of intermolecular forces. Latent stiffening occurred faster in gels hydrated with the phosphate buffer than with PBS, in buffer solutions containing lower salt concentrations (constant pH), and in gels of higher concentration or molecular weight PEG. Collectively, these observations suggest that electrostatic effects may influence the rate of latent stiffening in HAS-PEGDA, for example, by lowering the energy barrier to disulfide bonding.[4,47,50]

When fluorescein-*o*-acrylate was conjugated to the hydrogels in the place of PEGMA to block latent disulfide crosslinking, G′ at steady-state also decreased in a dose-dependent manner [Fig. 3(b)]. In addition, the concentration of residual, bound fluorescein was inversely related to G′ when HA-thiols (6 mM) were in molar excess of fluorescein-acrylates. The influence of the fluorescein-*o*-acrylate appeared to saturate around 7.5 mM, where both the residual fluorescence intensity and equilibrium stiffness plateaued [Fig. 3(b)]. Taken together, these findings indicate that the equilibrium stiffness can be tuned independently of initial gelation while concurrently tethering functional molecules to the hydrogel.

D. Introducing controlled bioactivity

Without the addition of peptide-ligands, HAS-PEGDA is non-cell-adhesive.[27–30,50] Therefore, cell adhesion was used for the proof-of-concept to validate that bioactivity could be introduced into the hydrogels (Fig. 4). Various ratios of the functional adhesive ligand (PEGMA-GRGDS) and inactive control peptide (PEGMA-SDGRG) were grafted to tune adhesion at a time point in between the two crosslinking reactions. In all conditions, the total concentration of PEGMA-peptide grafted to the hydrogels after 1 day of gelation was maintained in excess of remaining HA-thiols to completely block latent stiffening. For gels of constant

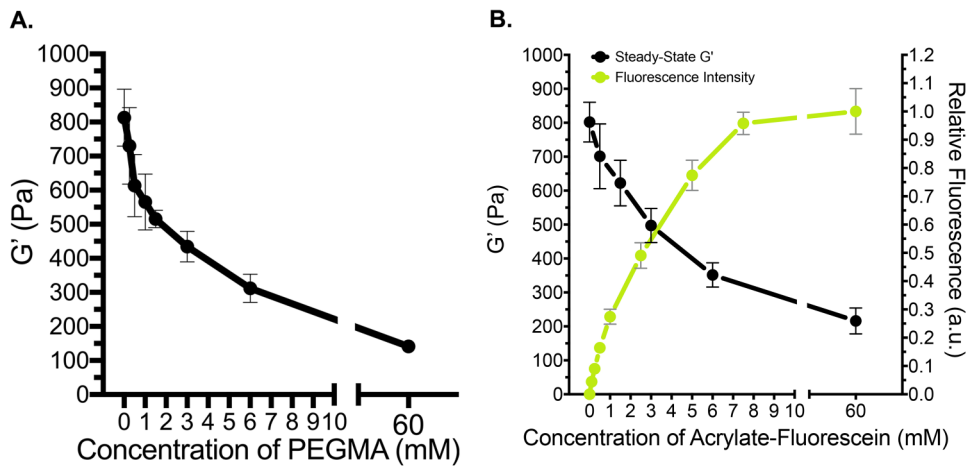

FIG. 3. Extent of latent stiffening can be controlled by targeting specific concentrations of HA-thiols after 1 day of gel maturation. (a) G′ at steady-state inversely relates to the concentration of PEGMA diffused into the hydrogel on 1 day of gelation. When PEGMA is presented in 10× molar excess (60 mM) of remaining HA-thiols (6 mM), G′ at steady-state is nearly identical to G′ after 1 day of gelation, indicating that disulfide crosslinking is completely blocked. (b) The residual fluorescence intensities ($\lambda_{ex}/\lambda_{em} = 490/520$ nm) of hydrogels grafted with fluorescein-*o*-acrylate inversely relate to G′ at steady-state, demonstrating that the final stiffness can be controlled independently of initial gelation while binding functional molecules to the network.

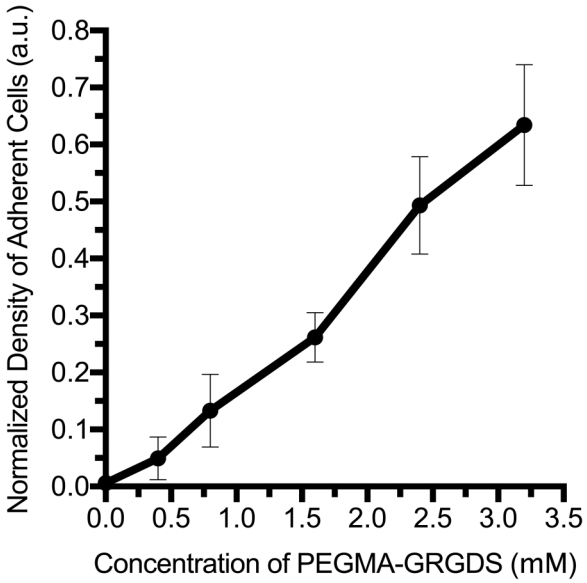

FIG. 4. For hydrogels of constant stiffness, adhesive ligand concentration controls the attachment and spreading of RDFs in a dose-dependent manner. The maximum concentration of the bound ligand in the hydrogels (x-axis) depends on both the relative ratio of the active ligand and the availability of HA-thiols in gels of 0.8% HA-S and 0.6% PEGDA after 1 day of gelation (~3.2 mM). For each condition, the average density of adherent cells was normalized to the initial cell seeding density of 5000 RDFs/well and is presented as normalized mean ± SEM for $n \geq 3$.

stiffness, the adhesive ligand concentration influenced both the density of adherent cells after 2 h (Fig. 4) and RDF morphology after 1 day *in vitro* [Figs. 5(a)–5(e)]. Without the addition of peptides, virtually no cells attached to gels [Fig. 5(a)], and few cells attached nonspecifically to gels quenched with the negative control peptide [Fig. 5(b)]. Hydrogels quenched with a 1:3 ratio of active ligand-to-inactive peptide were more adherent, and fibroblasts in these conditions were partially spread after day *in vitro 1* (DIV 1) [Fig. 5(c)]. Cells attached in the greatest numbers on hydrogels quenched with the active ligand [Fig. 5(d)]. These cells were also the most spread and exhibited stellate shapes. No significant differences were observed when a greater excess of active ligand (9 mM) was applied to the hydrogels [Fig. 5(e)]. This suggests that the wash steps were sufficient to remove unbound ligand, which would otherwise competitively inhibit cell adhesion.

E. Decoupling mechanical and bioactive signaling features

The heat maps in Fig. 6 demonstrate that stiffness and adhesive ligand concentration work in concert to influence both the adhesion of RDFs and their spreading areas. In each condition, stiffness was controlled by the concentration of PEGDA as HA-thiols were quenched with PEGMA-peptides

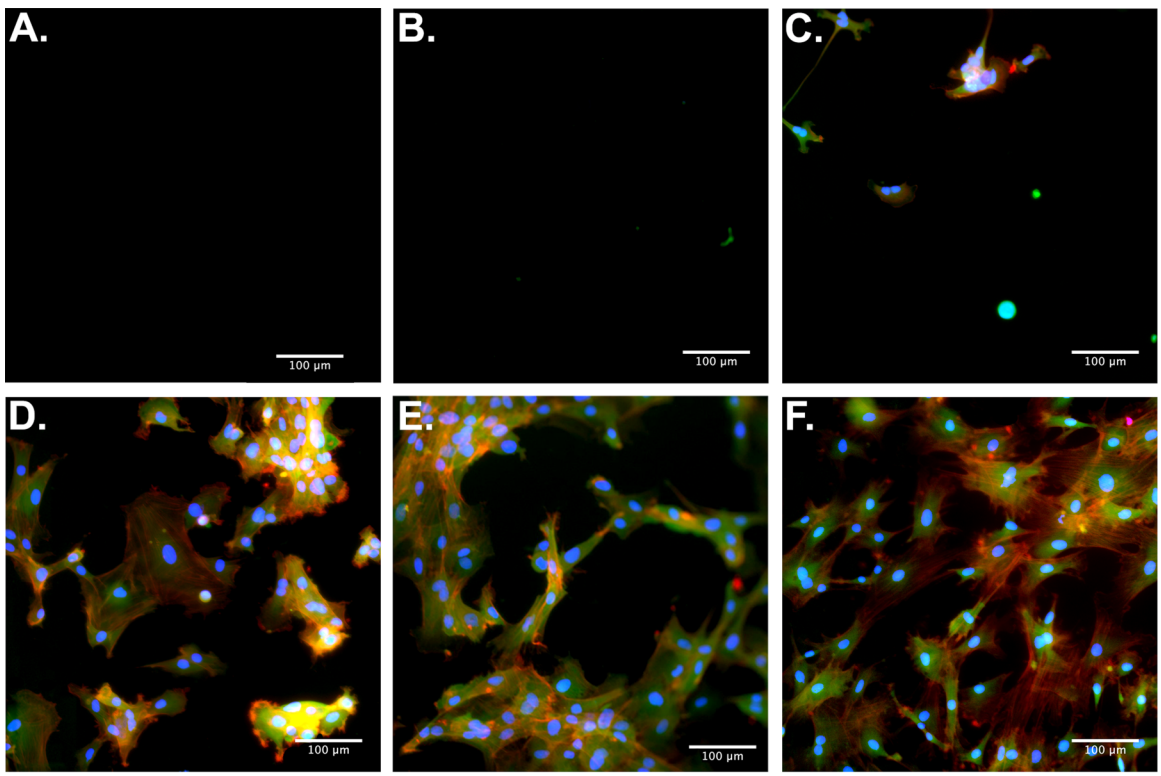

FIG. 5. (a)–(f) Images taken on DIV 1 with a 10× objective lens to visualize RDF cell bodies (endogenous GFP, green), F-actin stress fibers (TRITC-phalloidin, red), and cell nuclei (DAPI, blue). (a) There is virtually no cell attachment to gels without grafted peptide. (b) Very few cells attached to hydrogels quenched with the negative control peptide PEGMA-SDGRG (0 mM RGD), and of the cells that adhered, none had spread. (c) RDFs partially spread on hydrogels quenched with a 1:3 ratio of the active ligand to the inactive peptide (~0.8 mM RGD) and (d) RDFs exhibited stellate shapes on hydrogels quenched with the adhesive ligand PEGMA-GRGDS (~3.2 mM RGD). (e) No significant differences were observed when a greater excess of the active ligand (9 mM) had been applied to the hydrogels. (f) RDF attachment and spreading on positive control hydrogels of 2.0 mg/mL type-I bovine collagen.

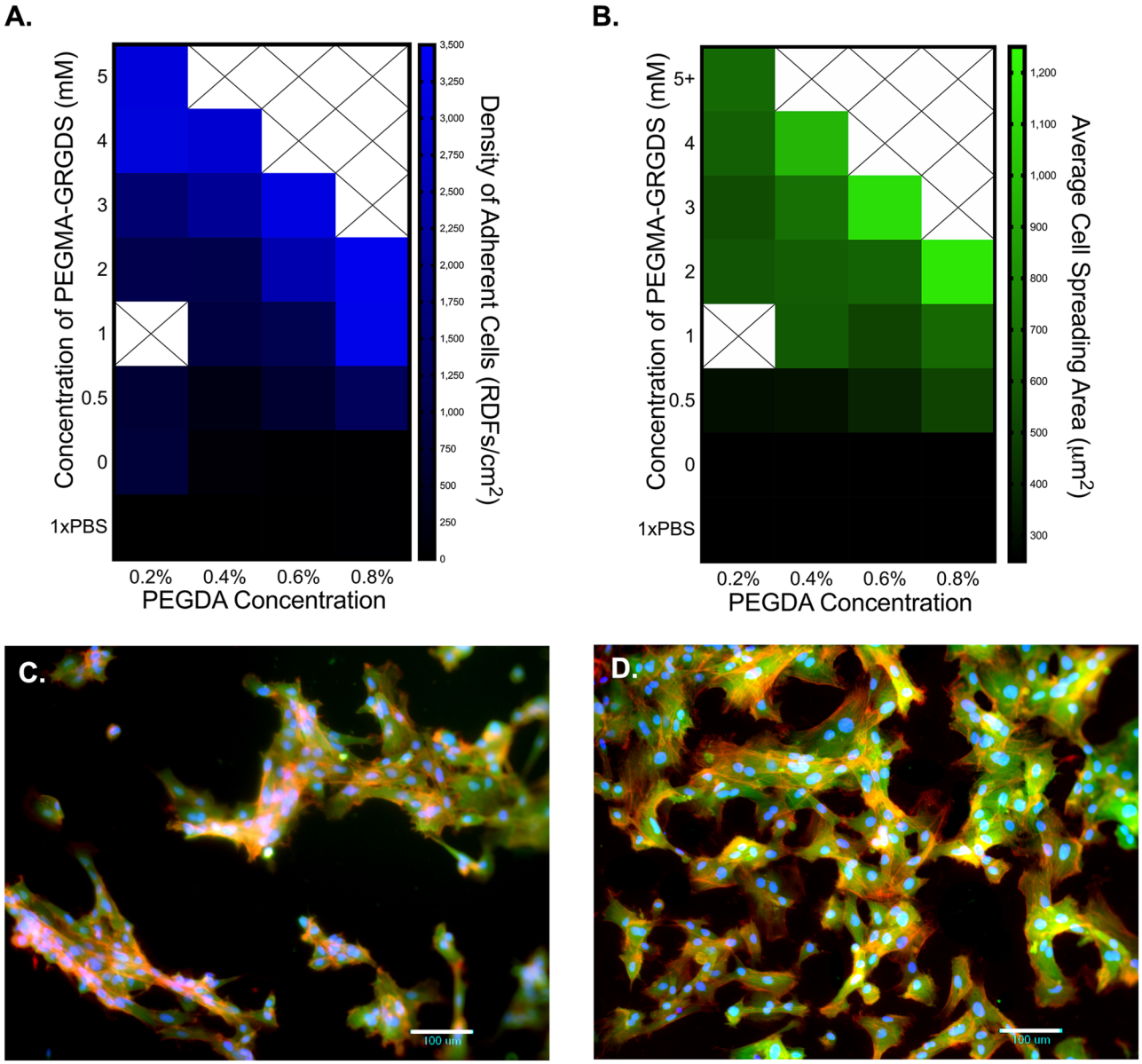

FIG. 6. RDF adhesion and morphology are codirected by matrix stiffness and adhesive ligand concentration. The average density of adherent cells and their morphologies directly relate to the concentration of PEGMA-GRGDS for gels of constant stiffness (columns) and to the PEGDA crosslinking density for gels of constant adhesivity (rows). (a) Mean density of adherent cells (RDFs/well). (b) Average cell spreading areas (μm^2/cell). (c) RDFs on 0.8% HA-S and 0.2% PEGDA hydrogels quenched with PEGMA-GRGDS. (d) RDFs on 0.8% HA-S and 0.8% PEGDA hydrogels quenched with PEGMA-GRGDS. Images were taken on DIV 1 with a 10× objective lens to visualize RDF cell bodies (green), F-actin stress fibers (red), and cell nuclei (blue).

prior to latent stiffening. Since the peptides target HA-thiols remaining after initial gelation, PEGDA concentration also influences the possible range of bound ligands. In general, the number of adherent cells was affected by both the concentration of PEGMA-GRGDS and the stiffness of the hydrogel [Fig. 5(a)]. For gels of constant stiffness (columns), cell attachment directly relates to the concentration of the adhesive ligand. Additionally, on gels of constant ligand density, cell adhesion relates to the stiffness of the substrate [Fig. 6(a) moving left-to-right across the rows]. For instance, in conditions of 2 mM PEGMA-GRGDS, fibroblast density on the stiffest hydrogels (0.8% PEGDA) was more than three times that of the most compliant hydrogels (0.2% PEGDA).

In addition to the number of cells, the concentrations of both PEGDA and the adhesive ligand influenced cell spreading, albeit to different extents [Fig. 6(b)]. For instance, on the most compliant gels (0.2% PEGDA), cell spreading areas were least affected by adhesive ligand concentrations [Fig. 6(b), column 1], despite these gels having the broadest range to graft bioactives (0–6 mM). On the slightly stiffer hydrogels formulated with 0.4% PEGDA, we observed broader ranges of cell spreading areas [Fig. 6(b), column 2], despite there being a narrower range to conjugate adhesive ligands (0–4.5 mM). In general, this trend continued for increasing concentrations of PEGDA. For example, the concentration of PEGMA-GRGDS in the 0.2% PEGDA

condition [Fig. 6(c)] is more than triple that of the 0.8% PEGDA condition, but cell density, spreading area, and stress fiber formation are more pronounced on the 0.8% PEGDA hydrogels [Fig. 6(d)]. These findings demonstrate the underlying concept that stiffness and ligand density work in concert to coordinate traction-based cell behaviors, including cell adhesion and spreading, and serve as a proof-of-principle to demonstrate that the mechanical and bioactive properties in HAS-PEGDA can be independently tuned to influence traction-based cell behaviors.

IV. CONCLUSIONS

This study describes several opportunities to manipulate ECM signaling features in HAS-PEGDA hydrogels. By leveraging the hydrogel's two cytocompatible crosslinking reactions, we demonstrate that the mechanical properties can be tuned across multiple time scales while introducing specific bioactivity. Non-cell-adhesive hydrogels are advantageous because they allow for the incorporation of precise densities and specificities of attachment ligands to influence cell-type-specific behaviors. The system described in this paper demonstrates how the initial crosslinking reaction of HA-S can be decoupled from the extent of latent stiffening to enable the full range of bioactives to be immobilized to HA-thiols without perturbing hydrogel gelation. Moreover, cellular interactions with the hydrogels validate that stiffness and ligand density are tunable in relevant ranges to influence cell behavior. Although the focus here was to manipulate mechanotransductive signaling, such as through cell adhesion and spreading, this template offers a versatile mechanism to tether other chemical signals including small molecules, biologics, and ECM components through primary amines. Given the time scales of crosslinking and gel maturation, and the potential to introduce different components at different locations with 3D bioprinting, this HAS-PEGDA approach may offer significant value as a bioink system.

ACKNOWLEDGMENTS

The authors would like to thank the National Institutes of Health (NIH) (No. NIH-NINDS1R01NS078385), Rutgers Biotechnology Training Program (No. NIH5T32GM008339-20), Rutgers Graduate Training in Emerging Areas of Precision and Personalized Medicine Program (No. P200A150131), and the Rutgers Neuroengineering Working Group (RUNEG) for support of this work.

[1]N. Savage, Nature **540**, S56 (2016).
[2]A. Munaz *et al.*, J. Sci. **1**, 1 (2016).
[3]B. Alberts *et al.*, *Molecular Biology of the Cell* (Garland Science, New York, 2002).
[4]J. Kuriyan, B. Konforti, and D. Wemmer, *The Molecules of Life Physical and Chemical Principles.* (Garland Science, Taylor & Francis Group LLC, New York, 2013).
[5]P. Lu *et al.*, Cold Spring Harbor Perspect. Biol. **3**, a005058 (2011).
[6]H. G. Sundararaghavan, S. N. Masand, and D. I. Shreiber, J. Neurotrauma **28**, 2377 (2011).
[7]G. P. Raeber, M. P. Lutolf, and J. A. Hubbell, Biophys. J. **89**, 1374 (2005).
[8]F. Gattazzo, A. Urciuolo, and P. Bonaldo, Biochim. Biophys. Acta **1840**, 2506 (2014).
[9]N. J. Walters and E. Gentleman, Acta Biomater. **11**, 3 (2015).
[10]S. N. Masand *et al.*, Biomaterials **33**, 790 (2012).
[11]H. G. Sundararaghavan, G. A. Monteiro, B. L. Firestein, and D. I. Shreiber, Biotechnol. Bioeng. **102**, 632 (2009).
[12]C. Grau-Monge *et al.*, Biomed. Mater. **12**, 1 (2017).
[13]B. D. Ratner, A. S. Hoffman, F. J. Schoen, and J. E. Lemons, *Biomaterials Science: An Introduction to Materials in Medicine* (Elsevier Academic, San Diego, 2004).
[14]N. Huebsch *et al.*, Nat. Mater. **9**, 518 (2010).
[15]S. Nemir, H. N. Hayenga, and J. L. West, Biotechnol. Bioeng. **105**, 636 (2010).
[16]O. Chaudhuri *et al.*, Nat. Mater. **15**, 326 (2016).
[17]J. R. García and A. J. García, Nat. Mater. **13**, 539 (2014).
[18]A. Chopra *et al.*, J. Biomech. **45**, 824 (2012).
[19]G. Bao and S. Suresh, Nat. Mater. **2**, 715 (2003).
[20]A. Tajik *et al.*, Nat. Mater. **15**, 1287 (2016).
[21]B. N. Mason, J. P. Califano, and C. A. Reinhart-king, "Matrix stiffness a regulator of cellular behavior and tissue formation," in *Engineering Biomaterials for Regenerative Medicine Novel Technologies for Clinical Applications*, edited by S. K. Bhatia (Springer Science+Business Media, LLC, New York, 2012), pp. 19–38.
[22]K. Ye *et al.*, Nano Lett. **15**, 4720 (2015).
[23]T. J. Kirby and J. Lammerding, Nat. Mater. **15**, 1227 (2016).
[24]V. H. Barocas and R. T. Tranquillo, J. Biomech. Eng. **119**, 137 (1997).
[25]E. A. Appel, B. L. Larson, K. M. Luly, J. D. Kim, and R. Langer, Adv. Healthcare Mater., **4**, 501 (2015).
[26]Y. Lei, S. Gojgini, J. Lam, and T. Segura, Biomaterials **32**, 39 (2011).
[27]J. Lam, N. Truong, and T. Segura, Acta Biomater. **10**, 1571 (2014).
[28]S. Khetan *et al.*, Nat. Mater. **12**, 458 (2013).
[29]K. Ghosh, X. Ren, X. Z. Shu, G. D. Prestwich, and R. A. F. Clark, Tissue Eng. **12**, 601 (2006).
[30]X. Z. Shu, Y. Liu, Y. Luo, M. C. Roberts, and G. D. Prestwich, Biomacromolecules **3**, 1304 (2002).
[31]X. Z. Shu, Y. Liu, F. Palumbo, and G. D. Prestwich, Biomaterials **24**, 3825 (2003).
[32]T. D. Mehra, K. Ghosh, X. Z. Shu, G. D. Prestwich, and R. A. F. Clark, J. Invest. Dermatol. **126**, 2202 (2006).
[33]K. Ghosh *et al.*, Biomacromolecules **6**, 2857 (2005).
[34]X. Z. Shu, Y. Liu, F. S. Palumbo, Y. Luo, and G. D. Prestwich, Biomaterials **25**, 1339 (2004).
[35]ESIBio. Hystem Hydrogel Kit, GS311 Technical Data Sheet. See: https://esibio.com/media/wysiwyg/esibio/documents/WEB_Rev._B_GS311_Hystem_7.5_Datasheet.pdf (last accessed January 16, 2019).
[36]J. P. Tam, C. R. Wu, W. Liu, and J. W. Zhang, J. Am. Chem. Soc. **113**, 6657 (1991).
[37]C. N. Yiannios and J. V. Karabinos, J. Org. Chem. **28**, 3246 (1963).
[38]G. W. Cline and S. B. Hanna, J. Org. Chem. **53**, 3583 (1988).
[39]S. Udenfriend *et al.*, Science **172**, 871 (1972).
[40]Sigma-Aldrich. Fluorescamine (F 9015) Product Information Sheet. See: https://www.sigmaaldrich.com/content/dam/sigma-aldrich/docs/Sigma/Product_Information_Sheet/f9015pis.pdf (last accessed January 16, 2019).
[41]G. A. Monteiro, A. V. Fernandes, H. G. Sundararaghavan, and D. I. Shreiber, Tissue Eng. A **17**, 1663 (2011).
[42]J. Schindelin *et al.*, Nat. Methods **9**, 676 (2012).
[43]J. L. Vanderhooft, M. Alcoutlabi, J. J. Magda, and G. D. Prestwich, Macromol. Biosci. **9**, 20 (2009).
[44]C. W. Macosko, *Rheology: Principles, Measurements, and Applications* (Wiley, New York, 1996).
[45]R. Banerjee, J. Biol. Chem. **287**, 4397 (2012).
[46]T. I. Zarembinski *et al.*, Acta Biomater. **10**, 94 (2014).
[47]L. A. H. Van Bergen, G. Roos, and F. De Proft, J. Phys. Chem. A **118**, 6078 (2014).
[48]M. Schäfer and S. Werner, Pharmacol. Res. **58**, 165 (2008).
[49]L. E. S. Netto *et al.*, Comp. Biochem. Physiol. C Toxicol. Pharmacol. **146**, 180 (2007).
[50]P. Y. Bruice, *Organic Chemistry* (Pearson, New York, 2011).
[51]M. J. Webber, E. A. Appel, E. W. Meijer, and R. Langer, Nat. Mater. **15**, 13 (2015).